



# HHS Public Access

Author manuscript

*Bioconjug Chem.* Author manuscript; available in PMC 2016 April 15.

Published in final edited form as:

*Bioconjug Chem.* 2015 April 15; 26(4): 660–668. doi:10.1021/bc500597y.

## Optical Imaging of Targeted $\beta$ -Galactosidase in Brain Tumors to Detect EGFR Levels

Ann-Marie Broome<sup>†,‡,§,\*</sup>, Gopal Ramamurthy<sup>†</sup>, Kari Lavik<sup>†</sup>, Alexander Liggett<sup>†</sup>, Ian Kinstlinger<sup>†</sup>, and James Basilion<sup>||,⊥,#</sup>

<sup>†</sup>Department of Radiology and Radiological Sciences, Medical University of South Carolina, Charleston, South Carolina 29425, United States

<sup>‡</sup>Center of Biomedical Imaging, Medical University of South Carolina, Charleston, South Carolina 29425, United States

<sup>§</sup>Department of Neurosciences, Medical University of South Carolina, Charleston, South Carolina 29425, United States

<sup>||</sup>Department of Biomedical Engineering, Case Western Reserve University, Cleveland, Ohio 44106, United States

<sup>⊥</sup>Case Center for Imaging Research, Case Western Reserve University, Cleveland, Ohio 44106, United States

<sup>#</sup>The NFCR Center for Molecular Imaging, Case Western Reserve University, Cleveland, Ohio 44106, United States

### Abstract

A current limitation in molecular imaging is that it often requires genetic manipulation of cancer cells for noninvasive imaging. Other methods to detect tumor cells *in vivo* using exogenously delivered and functionally active reporters, such as  $\beta$ -gal, are required. We report the development of a platform system for linking  $\beta$ -gal to any number of different ligands or antibodies for *in vivo* targeting to tissue or cells, without the requirement for genetic engineering of the target cells prior to imaging. Our studies demonstrate significant uptake *in vitro* and *in vivo* of an EGFR-targeted  $\beta$ -gal complex. We were then able to image orthotopic brain tumor accumulation and localization of the targeted enzyme when a fluorophore was added to the complex, as well as validate the internalization of the intravenously administered  $\beta$ -gal reporter complex *ex vivo*. After fluorescence imaging localized the  $\beta$ -gal complexes to the brain tumor, we topically applied a bioluminescent  $\beta$ -gal substrate to serial sections of the brain to evaluate the delivery and integrity of the enzyme. Finally, robust bioluminescence of the EGFR-targeted  $\beta$ -gal complex was captured within the tumor during noninvasive *in vivo* imaging.

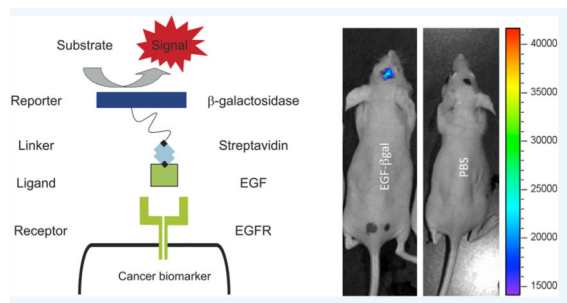
© 2015 American Chemical Society

\*Corresponding Author. broomea@muscc.edu. Office: 1-843-876-2481. Fax: 1-843-876-2469.

#### Author Contributions

The manuscript was written through contributions of all authors. All authors have given approval to the final version of the manuscript.

The authors declare no competing financial interest.



## INTRODUCTION

$\beta$ -Galactosidase ( $\beta$ -gal) is an enzyme that has been used heavily as a marker to detect gene expression, and several substrates exist to assay its presence in cells and tissue, including fixed tissue.<sup>1,2</sup> More recently investigators have sought to exploit the robust activity of  $\beta$ -gal enzyme for noninvasive imaging in biological systems that are genetically engineered to express  $\beta$ -gal.<sup>3–5</sup> Weissleder and co-workers have reported the use of DDAGO as an *in vivo* substrate for  $\beta$ -gal activity that fluoresces in the nearinfrared (NIR) making it ideal for detection of  $\beta$ -gal activity expressed by genetically engineered 9L glioma cells. Although the excitation and emission spectra of this agent overlap significantly, these investigators were able to demonstrate measurable fluorescence dependent on  $\beta$ -gal expression from engineered 9L glioma cells or cancer cells infected *in vivo* with a virus driving expression of  $\beta$ -gal. Blau and co-workers have taken a different approach to imaging  $\beta$ -gal activity noninvasively *in vivo*.<sup>4</sup> In these studies, they utilized sequential reporter-enzyme luminescence to detect  $\beta$ -gal activity using Lugal substrate. Lugal is a caged luciferase substrate that requires “uncaging” by  $\beta$ -gal to become a substrate for luciferase. Using this agent the investigators were able to detect luminescence *in vivo* only from cells that expressed both luciferase and  $\beta$ -gal enzymes. Further, they demonstrated that systemic administration of  $\beta$ -gal conjugated antibodies could be used to selectively label cells *in vivo* and after Lugal injection generate luminescence signal identifying the location of the cells using noninvasive bioluminescence imaging, as long as the targeted cells had been engineered to express luciferase.

Another approach for the development of activated MRI contrast agents is receptor-induced magnetization enhancement, or RIME.<sup>6,7</sup> This contrast agent consists of two parts, a gadolinium complex and a  $\beta$ -glucuronidase substrate ( $\beta$ -D-glucopyranuronic acid). Consequently,  $\beta$ -glucuronidase activity endogenously expressed within tumor tissues could be evaluated. A more recent example of this is by Hanaoka et al. in which  $\beta$ -gal is exploited to remove a galactopyranose-masking group allowing a strong interaction to occur between the gadolinium complex and albumin.<sup>8</sup> The result is a slower molecular tumbling rate, leading to a stronger relaxivity. Based on findings of different relaxivity gaps for MR contrast agents, several groups have developed probes to report on different microenvironment or enzyme expressions, including hypoxic conditions as well as peroxidase and esterase activity.<sup>9–14</sup>

Relevant to the techniques described within this work, Meade and co-workers also developed a modified sugar substrate containing a gadolinium chelate (EGadMe) to enhance the imaging contrast of  $\beta$ -gal in magnetic resonance imaging (MRI). In the absence of  $\beta$ -gal, EGadMe exhibits a water inaccessible conformation; in the presence of  $\beta$ -gal, the enzyme cleaves the sugar (galactopyranose) from EGadMe causing an increase in  $T_1$  relaxivity.<sup>15</sup> MRI was conducted in living *X. laevis* embryos transfected with plasmid DNA of the  $\beta$ -gal gene (*lacZ*) and showed significant signal intensity enhancement. However, there are limitations on requiring genetic manipulation of cancer cells for noninvasive imaging, and other methods to detect tumor cells in vivo using  $\beta$ -gal will be required. Here, we report the development of a platform system for linking  $\beta$ -gal to any number of different ligands or antibodies for in vivo targeting to tissue or cells, without the requirement for genetic engineering of the target cells prior to imaging.

For our studies  $\beta$ -gal has been engineered to contain a His tag for purification and a biotinylation signal.<sup>16</sup> Once expressed in bacteria, these proteins can be easily purified over a nickel column and then complexed via streptavidin (SA) to any ligands or antibodies to target the enzyme to biomarkers in vivo.<sup>16</sup> Administration of different fluorescent or bioluminescent substrates for  $\beta$ -gal can then be used to detect the location of the enzyme (Figure 1). In addition, we utilize a fluorescent marker conjugated on the SA to provide an additional means of gaining histological and cellular positional information.

We were interested in determining whether  $\beta$ -gal could be used to assess the expression of endogenous biomarkers in brain tumors that have been reported to be involved with malignant transformation and cancer growth. The most common gain of function mutation observed in invasive phenotypes associated with high-grade gliomas of the classical subtype, occurring in 30–50% of all glioblastomas, is the amplification and overexpression of the epidermal growth factor receptor (EGFR).<sup>17–21</sup> Tumors that overexpress EGFR have increased activity associated with uncontrolled cell growth accompanied by decreased apoptosis and increased angiogenesis and also activate other genes that promote cancer growth through such means as invasion and metastasis, as well as resistance to chemotherapy and radiotherapy.<sup>22–24</sup> Because of its relatively small size, we therefore utilized an epidermal growth factor (EGF) engineered peptide to target EGFR on the surface of brain tumor cells and demonstrate noninvasive imaging of EGFR expression.<sup>25</sup> Further, we are able to demonstrate that these complexes are able to detect differences in expression of EGFR between different brain tumors in vivo. The development of such a reporter provides the opportunity to, in the future, image multiple receptors by targeting the reporter enzyme to the surface receptor and then targeting an imageable substrate to a different cell surface receptor, thereby requiring the expression of two biomarkers to drive signal generation.

## RESULTS

$\beta$ -Galactosidase ( $\beta$ -gal) is a classic reporter enzyme used to examine the expression of various proteins in vitro and in vivo. The enzyme functions as a tetramer composed of 4 individual monomers with 5 domains. It is very robust such that its activity can be assayed even after fixation of cells. We wondered whether this robust reporter enzyme could be used

to measure the level of cell surface receptors present on brain tumors in an orthotopic mouse model of human brain tumors. Using molecular engineering techniques, full-length  $\beta$ -gal was engineered to have two tags: (1) His-tag for protein purification over an affinity column and (2) biotin-tag for complexing the  $\beta$ -gal to SA to form an imaging complex that can be delivered exogenously (Figure 1a).<sup>16</sup> We have used this construct to produce a platform-based approach for a molecular imaging strategy able to noninvasively measure the level of cell surface receptors expressed on tumors in vivo. As previously demonstrated, the constructs in Figure 1b can be synthesized, purified, and retain  $\beta$ -gal activity.<sup>16</sup> A control construct was also created which did not contain a targeting moiety and thus subject to clearance from the local environment (Figure 1c).

We first sought to demonstrate targeting of this construct outlined in Figure 1 to cells that express EGFR. The genetically modified  $\beta$ -gal was purified and concentrated prior to use. After confirmation of SA binding to  $\beta$ -gal, the complete EGF- $\beta$ -gal complex was prepared by combining biotinylated EGF peptide and biotinylated- $\beta$ -gal and mixing them in the presence of Alexa 647-conjugated SA at molar ratios of 1:3:1. Constructs were then added to Gli36 5 cells, which overexpress EGFR in vitro, and binding and uptake of the EGF- $\beta$ -gal complex was monitored by fluorescence microscopy using the fluorophore-labeled SA contained within the complex (Figure 2a). The construct seemed to concentrate in discrete vesicles surrounding the perinuclear region of the cell as observed in Figure 2a and b. Once internalized into the cell, the  $\beta$ -gal retained enzyme activity as shown by staining with the  $\beta$ -gal substrate, 5-bromo-4-chloro-3-indolyl- $\beta$ -D-galacto-pyranoside (X-gal) (Figure 2b). Internalization of the EGFR-targeted  $\beta$ -gal complexes was competitively inhibited by full-length EGF (50% inhibition) within a 4 h incubation period (Figure 2c).

We next tested the utility of the construct to accumulate in tumors expressing EGFR using an orthotopic mouse model for brain tumors. Glioma cells, Gli36 5, were stereotactically implanted in the brains of mice and grown for approximately 10 days as per IUCAC approved protocols. Mice were intravenously injected with 1 mg kg<sup>-1</sup> body weight of either EGF- $\beta$ -gal (targeted) or B- $\beta$ -gal (nontargeted), both of which incorporated Alexa 647-labeled SA to easily visualize targeted-complex uptake following tissue preparation (Figure 3a). Targeted- $\beta$ -gal crossed the blood-brain-tumor-barrier (BBTB) as measured by fluorescence molecular tomography in living mice (Figure 3b). Approximately 3–5% (~133 nM) of the injected dose accumulated within the tumor within 4 h. After 4 h, the mice were euthanized and the brains were removed and imaged whole and then serially transected into 2 mm sections and imaged again ex vivo using a Maestro fluorescence imaging system (Figure 3c, top panels). EGF- $\beta$ -gal specifically accumulates in the tumor within 4 h. In contrast, nontargeted B- $\beta$ -gal did not accumulate in the tumor as indicated by a lack of fluorescent signal, but presumably remained in the ventral cerebral and cerebellar arteries of the brain (Figure 3c, bottom panels).

Serial sections of the brains were cryosectioned and counterstained with DAPI to delineate cell nuclei. Fluorescence images captured at 100 $\times$  magnification clearly showed significant EGF- $\beta$ -gal uptake within the tumor and internalization within the cells' cytoplasm. Cryosections of brain containing the tumor region were then counterstained with anti-EGFR (Figure 3d) or antivimentin (Figure 3e) and visualized using epifluorescence microscopy.

These studies indicated that EGFR is heterogeneously expressed within the tumor (green) and that targeted- $\beta$ -gal complex (red) accumulates specifically in glioma cells overexpressing EGFR (Figure 3d). Vimentin staining, a standard pro-invasive intermediate filament tumor marker, identified implanted cells within the orthotopic mouse model which were of human origin, i.e., Gli36 5 cells, and demonstrated that targeted- $\beta$ -gal complex (red) only colocalized within human cells expressing vimentin (green) (Figure 3e). Little to no  $\beta$ -gal complex was found within other regions of the brain (data not shown).

We then determined whether  $\beta$ -gal activity was maintained by the targeted complex. For these studies, orthotopic brain tumors implanted as described above were used. After approximately 10 days of growth, tumors were harvested by removing the intact mouse brain and then sectioning it into 2mm sections. Following sectioning, a bioluminescent  $\beta$ -gal substrate, Galacto-Light Plus,<sup>26</sup> was topically applied to the ex vivo brain serial sections to evaluate the delivery and integrity of enzyme across the BBTB (Figure 4a). Further, the targeting ability and enzymatic activity in Gli36 5-derived brain tumors, expressing high levels of EGFR, was compared to brain tumors implanted with U87 cells expressing low levels of EGFR. Robust bioluminescence was captured within the tumor overexpressing EGFR after 3 min, indicating that  $\beta$ -gal maintained its activity. Minimal  $\beta$ -gal activity was observed in U87-derived tumors, which express very low levels of the EGFR protein as previously determined by Western blot.<sup>27</sup> The luminescence was quantified and Gli36 5 tumors possessed 3–4-fold more enzymatic activity than U87 tumors (Figure 4b). Qualitatively this correlated well with the increase in average fluorescence intensity recorded between Gli36 5 tumors and U87 tumors. Tumor cryosections counterstained with EGFR antibody (green) and DAPI (blue) demonstrated the differences in both the level of EGFR expression and EGFR-targeted uptake of the  $\beta$ -gal complex within the two tumor types, high EGFR expression and low EGFR expression, respectively (Figure 4c). Western blot analysis confirmed the higher expression levels of EGFR observed in Gli36 5 cells versus U87 cells.<sup>27</sup>

The next step in these studies was to demonstrate that complex formation could be imaged noninvasively in living mice. Mice containing orthotopically implanted Gli36 5 cells were intravenously injected with 1 mg kg<sup>-1</sup> body weight of EGF- $\beta$ -gal (Figure 5a). Four hours later, Galacto-Light Plus, bioluminescence  $\beta$ -gal substrate, was stereotactically injected into the brain cavity through the original burr-hole used to implant the tumors. Targeted- $\beta$ -gal crossed the BBTB as measured and quantified by bioluminescence imaging in living mice (Figure 5b). Little to no bioluminescence was observed in sham treated mice (PBS). Stereotactic injection was utilized, in this case, as the substrate in our hands was found to be toxic upon systemic injection. Development of less toxic  $\beta$ -gal-activatable substrates is underway.

## DISCUSSION

$\beta$ -Gal is a very robust enzyme whose activity is maintained under a variety of different conditions, including tissue fixation, which is why it has been so widely selected for decades by molecular biologists as a tool to measure gene expression in several different settings. Many reporter substrates exist for this enzyme, but most are limited to histological or in

vitro use. Recently, several investigators have demonstrated the use of  $\beta$ -gal as a marker for noninvasive imaging of gene expression using MRI,<sup>15,28</sup> bioluminescence,<sup>4,26</sup> and NIRF imaging.<sup>3</sup> Although each technique is unique in its derivation and application, all share the characteristic of requiring genetic manipulation of target cells to allow in vivo measurement of  $\beta$ -gal activity. For the methods of both Mason and Weissleder,  $\beta$ -gal activity is directly measured after it is expressed in the target cells, which then can activate a substrate to generate bioluminescence or fluorescence in vivo, respectively. In another iteration, Meade and co-workers use a caged gadolinium, which is conformationally exposed after  $\beta$ -gal cleavage, to generate signal enhancement for MRI.<sup>15</sup> In these studies, transfection of a plasmid containing the 3000 bp  $\beta$ -gal sequence was required to generate ~88–352 copies of the plasmid per cell at the 100 000-cell stage. For MRI, this required that many millions of  $\beta$ -gal enzymes needed to be expressed in the *Xenopus* embryo of 1 mm diameter to achieve a significant enhancement of the T<sub>1</sub> signal.

Blau and co-workers use  $\beta$ -gal enzyme to activate a caged luciferase substrate measuring  $\beta$ -gal activity by the “un-caging” of the substrate, which is then used by luciferase to generate a signal.<sup>4</sup> In this paradigm, the target tissue or cells need to express luciferase, but it is not required that they express  $\beta$ -gal. Interestingly, they demonstrated that exogenous  $\beta$ -gal could be administered as an antibody conjugate to an animal, targeting it to cells that express luciferase. After administration of the caged luciferase, Lugal, the compound is converted in situ to luciferin, which enters the cells and serves as a substrate for luciferase expressed within the cells.<sup>4</sup>

We have developed a technology for noninvasive assessment by  $\beta$ -gal, which does not require genetic engineering of an animal model expressing  $\beta$ -gal. In our system, an engineered  $\beta$ -gal enzyme is purified from *E. coli*. Because of a biotinylation element contained within the N-terminal end of the enzyme,<sup>16</sup> the protein is able to complex with SA and another biotinylated ligand. This complex can be directly injected into mice bearing a brain tumor and accumulates within tumors dependent on the number of surface proteins (targets) that the tumor cells express. Injection of a  $\beta$ -gal bioluminescent substrate, such as Galacto-Light Plus, allows quantitative readout of  $\beta$ -gal activity.

The use of an injectable  $\beta$ -gal complex eliminates many of the restrictions for previous applications to exploit  $\beta$ -gal as a biomarker (i.e., genetic manipulation of target tissue) and moves  $\beta$ -gal into the realm of an imaging tool that can be used to identify the location of biomarkers without any a priori knowledge of the location of their expression. A combination of both fluorescent marker and enzymatic reporter (bioluminescence) in one complex could facilitate the study of the intended target at different spatial resolution and intensity scales. Multiple approaches could be used to follow a molecular target or pathway. Additionally, the utilization of  $\beta$ -gal, as described, provides an opportunity to begin to utilize multiple receptors expressed on the same cell surface to drive signal generation. In this scenario,  $\beta$ -gal would be targeted to the cell surface using one biomarker and an imageable substrate targeted to a different receptor on the cell surface allowing for activation by localized  $\beta$ -gal. One interesting avenue is the development of activatable MR contrast agents that could be directed to the cell surface for  $\beta$ -gal activation that would allow for high-resolution imaging of targeted tissues. Further, this approach potentially increases the

sensitivity for such detection as the use of a bioluminescence substrate eliminates autofluorescence background, thereby reducing signal-to-noise (SNR) for many fluorescence-based noninvasive imaging approaches. Typically, fluorescence is coupled with bioluminescence to provide an additional means to gain more histological and cellular positional information.

The studies described here also potentially provide another approach to novel antibody-directed enzyme pro-drug therapy (ADEPT) approach to chemotherapy for cancer.<sup>29–32</sup> In the case of ADEPT,  $\beta$ -gal is utilized to activate a pro-drug therapy in a two-step approach much like that proposed in this study. In the first step, a drug-activating enzyme is targeted and expressed in tumors. In the second step, a nontoxic pro-drug, a substrate of the exogenous enzyme that is now localized to tumor tissues, is administered systemically. The result is that a systemically administered pro-drug can be converted to high local concentration of an active anticancer drug in tumors by a targeted enzyme, such as  $\beta$ -gal. With this platform, a personalized approach to patient care can also be developed.  $\beta$ -gal can be targeted to a patient's cancer utilizing *any cell surface marker* identified in a genomic screen as specifically overexpressed in the particular cancer, followed by pro-drug therapy. The complexes demonstrated here provide a robust platform for the targeting of  $\beta$ -gal (or other enzymes) to any number of different biomarkers using endogenous ligands, small molecule ligands, as well as antibodies. This potentially provides a means to target cell surface proteins for which no antibodies exist or for which conjugation chemistries destroy enzymatic activity of the prodrug-activating enzyme. Indeed for  $\beta$ -gal, several pro-drug substrates do exist, which, when activated, generate toxicity for cancer cells both in vitro and in vivo.<sup>32–35</sup>

In summary, we have developed a novel conjugation of engineered  $\beta$ -gal that allows for rapid purification and complex formation of the enzyme with virtually any biotinylated ligand or antibody and application of the complex to cells, both in vitro and in vivo allowing for rapid identification of target expression. The direct approach of administering targeted  $\beta$ -gal complexes combined with the use of bioluminescent substrate eliminates the need for genetic manipulation of the target tissue and rapid readout of target expression. While demonstrated for  $\beta$ -gal, there is no reason that this approach cannot be used for other enzymes and it has the potential to also be used to activate pro-drugs once existence of the targeted biomarker is confirmed by imaging.

## EXPERIMENTAL SECTION

### $\beta$ -Galactosidase Complex Creation, Propagation, and Purification

DNA encoding the full-length  $\beta$ -gal from the pSV- $\beta$ -gal plasmid (Promega; Madison, WI) was amplified by PCR using plasmid template and primers that introduce flanking restriction enzyme sequences. The PCR product was ligated into a pHAT10 vector (Clontech; Mountain View, CA) containing a suitable antibiotic selectable marker for bacterial propagation. The resulting coding sequence, consisting of the His-tag and full-length  $\beta$ -gal, was excised from the vector and inserted into the pAN4 vector (Avidity; Aurora, CO). The pAN4 vector was used to express a single N-terminal biotin–protein fusion.

Luria–Bertani (LB) broth (5 mL) containing ampicillin (50 mg mL<sup>-1</sup>) was inoculated with a bacterial scrape (~25 mL) containing full-length β-gal plasmid and allowed to grow overnight (18–20 h) in an incubator orbital shaker at 37 °C. Following the growth period, LB broth (1 L) with ampicillin (50 mg mL<sup>-1</sup>) was inoculated with the 5 mL overnight growth and placed in the incubator/orbital shaker at 37 °C until an absorbance of 0.4 was observed at 600 nm (5.5 h). The bacterial culture was then induced with 1 mM IPTG. The IPTG-induced culture was grown in an incubator/orbital shaker at 37 °C until a reading between 0.8 and 1.0 was observed at absorbance 600 nm (6 h). Upon completion, the cells were pelleted and the supernatant discarded. The cell pellet was lysed with lysozyme at room temperature for 20 min and then stored at –80 °C until purification.

β-Gal was purified from contaminating bacterial cell degradation products and other particles using affinity chromatography. The whole cell lysate was thawed at 37 °C, sonicated, and centrifuged. The lysate was passed over a nickel Talon affinity column (Clontech; Mountain View, CA) using gravity flow. The column was washed twice with extraction buffer [50 mM NaHPO<sub>4</sub>, pH 7; 300 mM NaCl in ddH<sub>2</sub>O]. The Histagged protein was eluted off the column in 0.5 mL fractions with elution buffer [0.15 M imidazole in extraction buffer]. Each fraction was analyzed for the presence and concentration of purified protein using standard protein analysis (Bio Rad DC Protein Assay kit; Bio Rad; Hercules, CA) and immunoblot analysis with anti-His (Upstate, Billerica, MA) and HRP-conjugated SA (Chemicon; Temecula, CA). Fractions containing the desired protein were combined, dialyzed against PBS, and stored at 4 °C.

### Targeted-Reporter Complex Assay for Live Cells

Biotinylated EGF for the EGFR was linked to biotinylated β-gal using fluorophore-conjugated SA. Ligand, linker, and reporter fragment were mixed in a molar ratio 1:1:3 at room temperature for 1 h. Excess D-biotin was added to block any remaining unbound SA sites. In the case of control assays, untargeted reporter complex was prepared with D-biotin, in place of the ligand, mixed with linker and reporter fragment in a molar ratio 1:1:3. The ligand-complex was then diluted to 500 mL with cell feeding media (DMEM, 10% fetal bovine serum, 1% penicillin–streptomycin) and added directly to coverslips seeded with cells overexpressing human EGFR. Cells were incubated with EGF ligand-complex for 1 h at 37 °C. The cells were then fixed with 4% paraformaldehyde, rinsed with X-gal wash buffer, and stained overnight at 37 °C with 1 mg mL<sup>-1</sup> X-gal (5-bromo-4-chloro-3-indolyl-β-D-galactopyranoside; Sigma; St Louis, MO, USA) in 5 mM K<sub>3</sub>Fe(CN)<sub>6</sub>, 5 mM K<sub>4</sub>Fe(CN)<sub>6</sub>, and 2 mM MgCl<sub>2</sub> in PBS. Cells were rinsed twice with PBS for 5 min. Images were captured by a Retiga EXi camera connected to a Leica DM4000 B upright microscope (Leica Microsystems; Wetzlar, Germany).

### Immunofluorescence Staining of Targeted-Reporter Complex

Biotinylated EGF was linked to biotinylated β-gal using fluorophore-conjugated SA. Ligand, linker, and reporter fragment were mixed in a molar ratio 1:1:3 at room temperature for 1 h. Excess D-biotin was added to block any remaining unbound SA sites. In the case of control assays, untargeted reporter complex was prepared with D-biotin, in place of the ligand, mixed with linker and reporter fragment in a molar ratio 1:1:3. The ligand-complex was then

diluted to 500 mL with cell feeding media (DMEM, 10% fetal bovine serum, 1% penicillin–streptomycin) and added directly to coverslips seeded with cells overexpressing human EGFR. Cells were incubated with EGF ligand-complex for 1 h at 37 °C. For competition assays, cells were incubated with a combination of EGF- $\beta$ -gal and either 200 nM or 1000 nM full-length EGF for 4 h. The cells were then fixed with 4% paraformaldehyde, rinsed with PBS, and blocked with 1% host serum for 30 min at room temperature. Coverslips were incubated with primary antibody at room temperature for 2 h. Antibodies used were mouse anti-EGFR (1:100 dilution; Dako; Carpinteria, CA), mouse anti-EEA1 (1:100 dilution; Cell Signaling Technology; Danvers, MA), rabbit anti-Lamp2 (1:500 dilution; Sigma-Aldrich; St. Louis, MO), and rabbit anti-Rab9 (1:500 dilution; Sigma-Aldrich; St. Louis, MO). The coverslips were then rinsed with PBS and counterstained with 2-(4-amidinophenyl)-6-indolecarbamide dihydrochloride (DAPI) for 10 min at room temperature to visualize the nuclei. After a final rinse with PBS, the coverslips were mounted using Fluor-Mount aqueous media, sealed with nail polish, and observed using epifluorescence microscopy. Relative fluorescence intensities were calculated using *ImageJ* software (NIH, MD).

### Orthotopic Brain Tumor Implantation

Athymic nude female mice (*nu/nu*, 6–8 weeks at time of surgery) were bred and maintained at the Animal Resource Center at Case Western Reserve University. All procedures were performed aseptically according to Institutional Animal Care and Use Committee (IACUC) approved protocols. For brain tumor implants, mice were anesthetized by intraperitoneal injection of 50 mg kg<sup>-1</sup> ketamine:xylazine and fitted into a stereotaxic rodent frame (David Kopf Instruments; Tujunga, CA). A small incision was made just lateral to midline to expose the bregma suture. A small (1.0 mm) burr hole was drilled at AP = +1, ML = -2.5 from bregma. Glioblastoma cells were slowly deposited at a rate of 1  $\mu$ L per minute in the right striatum at a depth of -3 mm from dura with a 10 mL Hamilton syringe (26G blunt needle; Fisher Scientific; Waltham, MA). The needle was slowly withdrawn and the incision was closed with 2–3 sutures. For flank tumor implants, mice were anesthetized with inhaled isoflurane:oxygen for immobilization. The Matrigel:cell mixture was loaded into a 1 mL syringe fitted with a 26-gauge needle and kept on ice. The mixture was injected subcutaneously in the right flank region of the mouse. The needle was withdrawn and the animal was returned to the cage for daily monitoring.

### Small Animal in Vivo Fluorescence Imaging

EGFR-targeted  $\beta$ -gal (EGF- $\beta$ -gal) or nontargeted  $\beta$ -gal (B- $\beta$ -gal) (1 mg kg<sup>-1</sup> body weight) was intravenously injected into mice harboring orthotopic brain tumors (*N* = 3 for each group). After 4 h of circulation, fluorescent molecular tomographic images were obtained using FMT2500 (PerkinElmer; Waltham, MA) and three-dimensional reconstructions of fluorescent signals were acquired using the accompanying software *TrueQuant*. Quantitative fluorescent signals for Alexa 647 were calibrated per manufacturer's instructions using the 635-channel. Region of interest (ROI) was assigned based on the precise placement of cells during implantation at 3–4mm into the brain. ROI was corroborated with fluorescent signals from ex vivo imaging.

Fluorescent multispectral images (647 nm) were obtained using the Maestro In Vivo Imaging System (CRi, Inc.; Woburn, MA) after the brains were removed. A band-pass filter appropriate for the Cy5 (yellow filter set, Ex 575–605 nm, Em 645; acquisition settings 630–850) was used for emission and excitation light, respectively. The tunable filter was automatically stepped in 10 nm increments while the camera captured images at a constant exposure of 1000 ms. The brains were then serially sectioned and reimaged to more precisely identify the tumor region. To compare signal intensities, ROI were selected over the entire treated area (tumor or nontumor) and the change in fluorescence signal over baseline was determined. The spectral fluorescent images consisting of autofluorescence spectra and imaging probe were captured and unmixed based on their spectral patterns using commercially available software (*Maestro* software v 2.4.0; CRi, Inc.; Woburn, MA). Spectral libraries were generated by assigning spectral peaks to the tissue background fluorescence, background from the imaging stage, and probe within tumor at maximal activation. Total signal in the ROI in photons measured at the surface of the brain was divided by the area in order to compare between animals and imaging experiments.

### Small Animal in Vivo Bioluminescence Imaging

Gli36 5 or U87 cells were stereotactically implanted in the brains of mice and grown for 10 days as per IUCAC approved protocols. EGFR-targeted  $\beta$ -gal (EGF- $\beta$ -gal; mice  $N = 5$ ) or nontargeted  $\beta$ -gal (B- $\beta$ -gal; mice  $N = 3$ ) ( $1\text{ mg kg}^{-1}$  body weight) was intravenously injected into mice harboring orthotopic brain tumors and allowed to circulate for 4 h. Mice were anesthetized with isoflurane and the substrate mixture, Galacto-Light Plus, 1,2-dioxetane substrates (Tropix; Bedford, MA, USA) and a light-emission accelerator containing a polymeric enhancer (Accelerator-II), was stereotactically injected into the brain cavity through the original burr-hole used to implant the tumors with a 26-gauge needle immediately after the 4 h circulation time. Imaging of  $\beta$ -gal was performed using the Xenogen IVIS 200 in vivo imaging system (Xenogen; Caliper Life Sciences; Hopkinton, MA) within 0.5 min after application. No animals died as a result of imaging or locally administered substrate treatment. Ex vivo bioluminescence imaging of isolated organs was performed immediately after euthanasia of the animals. Dissected brains were placed on a sheet of black background and imaged with IVIS 200. Luminescence for  $\beta$ -gal was determined 3 min after the topical addition of 100 mL Galacto-Light Plus reagent and Accelerator-II. Relative luminescence was quantitated by creating a ROI over the brain tumor and expressed as photons  $\text{s}^{-1} \text{ cm}^{-2}$ . To standardize the data, light emission was quantified from the same surface area for each brain. Corresponding gray-scale photographs and color luminescence images were superimposed and analyzed using *Living Image* analysis software v 3.1 (Xenogen). The brains were then fixed in 4% paraformaldehyde, cryo-preserved in 30% sucrose, and frozen in optimum cutting temperature compound (OCT) for cryosectioning (Leica CM3050S). Sections were collected serially at 10 or 25  $\mu\text{m}$  cut directly on to slides and stored at  $-80^\circ\text{C}$  until immunohistochemical staining. Cryosections of the tumor region were then counterstained with DAPI, mouse anti-EGFR (1:100 dilution; Dako; Carpinteria, CA), or rabbit antivimentin (1:500 dilution; LabVision; Fremont, CA), and visualized using fluorescence microscopy.

## ACKNOWLEDGMENTS

This work was supported by the National Foundation for Cancer Research (to J.P.B.) and a fellowship award (to A.M.B.). The project described was also supported by Grant Number K01EB006910 (to A.M.B.) from the National Institute of Biomedical Imaging and Bioengineering and by the Department of Defense Peer Reviewed Cancer Research Program Idea Award Grant Number W81XWH-11-1-0386 (to A.M.B.). The content and views are solely the responsibility of the authors and do not necessarily represent the official views of the National Institute of Biomedical Imaging and Bioengineering or the National Institutes of Health or the US Army or the Department of Defense.

## ABBREVIATIONS

<b>ADEPT</b>	antibody-directed enzyme pro-drug therapy
<b>B</b>	biotin
<b>β-gal</b>	beta-galactosidase
<b>BBB</b>	blood brain barrier
<b>BBTB</b>	blood brain tumor barrier
<b>DAPI</b>	4', 6-diamidino-2-phenylindole
<b>DDAGO</b>	9 <i>H</i> -(1, 3-dichloro-9, 9-dimethylacridin-2-one-7-yl) β-D-galactopyranoside
<b>EGF</b>	epidermal growth factor
<b>EGFR</b>	epidermal growth factor receptor
<b>GBM</b>	glioblastoma multiform
<b>IUCAC</b>	Institutional Use and Care Animal Committee
<b>MRI</b>	magnetic resonance imaging
<b>NIR</b>	near-infrared
<b>NIRF</b>	near-infrared fluorescence
<b>PBS</b>	phosphate buffered saline
<b>ROI</b>	region of interest
<b>SA</b>	streptavidin
<b>X-gal</b>	5-bromo-4-chloro-3-indolyl-β-D-galactoside
<b>SNR</b>	signal-to-noise ratio

## REFERENCES

1. Flanagan WM, Wagner EK. A bi-functional reporter plasmid for the simultaneous transient expression assay of two herpes simplex virus promoters. *Virus Genes*. 1987; 1(1):61–71. [PubMed: 2854322]
2. Jain C. New improved lacZ gene fusion vectors. *Gene*. 1993; 133(1):99–102. [PubMed: 8224902]
3. Tung CH, Zeng Q, Shah K, Kim DE, Schellingerhout D, Weissleder R. In vivo imaging of beta-galactosidase activity using far red fluorescent switch. *Cancer Res*. 2004; 64(5):1579–1583. [PubMed: 14996712]

4. von Degenfeld G, Wehrman TS, Blau HM. Imaging beta-galactosidase activity in vivo using sequential reporter-enzyme luminescence. *Methods Mol. Biol.* 2009; 574:249–259. [PubMed: 19685314]
5. Wehrman TS, von Degenfeld G, Krutzik PO, Nolan GP, Blau HM. Luminescent imaging of beta-galactosidase activity in living subjects using sequential reporter-enzyme luminescence. *Nat. Methods.* 2006; 3(4):295–301. [PubMed: 16554835]
6. Chen SH, Kuo YT, Singh G, Cheng TL, Su YZ, Wang TP, Chiu YY, Lai JJ, Chang CC, Jaw TS, Tzou SC, Liu GC, Wang YM. Development of a Gd(III)-based receptor-induced magnetization enhancement (RIME) contrast agent for beta-glucuronidase activity profiling. *Inorg. Chem.* 2012; 51(22):12426–12435. [PubMed: 23116118]
7. Aime S, Gianolio E, Terreno E, Giovenzana GB, Pagliarin R, Sisti M, Palmisano G, Botta M, Lowe MP, Parker D. Ternary Gd(III)L-HSA adducts: evidence for the replacement of inner-sphere water molecules by coordinating groups of the protein. Implications for the design of contrast agents for MRI. *J. Biol. Inorg. Chem.* 2000; 5(4):488–497. [PubMed: 10968620]
8. Hanaoka K, Kikuchi K, Terai T, Komatsu T, Nagano T. A Gd<sup>3+</sup>-based magnetic resonance imaging contrast agent sensitive to beta-galactosidase activity utilizing a receptor-induced magnetization enhancement (RIME) phenomenon. *Chemistry.* 2008; 14(3):987–995. [PubMed: 17992679]
9. Breckwoldt MO, Chen JW, Stangenberg L, Aikawa E, Rodriguez E, Qiu S, Moskowitz MA, Weissleder R. Tracking the inflammatory response in stroke in vivo by sensing the enzyme myeloperoxidase. *Proc. Natl. Acad. Sci. U.S.A.* 2008; 105(47):18584–18589. [PubMed: 19011099]
10. Gulaka PK, Rojas-Quijano F, Kovacs Z, Mason RP, Sherry AD, Kodibagkar VD. GdDO3NI, a nitroimidazole-based T1MRI contrast agent for imaging tumor hypoxia in vivo. *J. Biol. Inorg. Chem.* 2014; 19(2):271–279. [PubMed: 24281854]
11. Querol M, Chen JW, Weissleder R, Bogdanov A Jr. DTPA-bisamide-based MR sensor agents for peroxidase imaging. *Org. Lett.* 2005; 7(9):1719–1722. [PubMed: 15844889]
12. Iwaki S, Hanaoka K, Piao W, Komatsu T, Ueno T, Terai T, Nagano T. Development of hypoxia-sensitive Gd<sup>3+</sup>-based MRI contrast agents. *Bioorg. Med. Chem. Lett.* 2012; 22(8):2798–2802. [PubMed: 22424977]
13. Giardiello M, Lowe MP, Botta M. An esterase-activated magnetic resonance contrast agent. *Chem. Commun. (Cambridge).* 2007; 39:4044–4046. [PubMed: 17912410]
14. Touti F, Maurin P, Hasserodt J. Magnetogenesis under physiological conditions with probes that report on (bio-)chemical stimuli. *Angew. Chem. Int. Ed.* 2013; 52(17):4654–4658.
15. Urbanczyk-Pearson LM, Meade TJ. Preparation of magnetic resonance contrast agents activated by beta-galactosidase. *Nat. Protoc.* 2008; 3(3):341–350. [PubMed: 18323804]
16. Broome AM, Bhavsar N, Ramamurthy G, Newton G, Basilion JP. Expanding the utility of beta-galactosidase complementation: piece by piece. *Mol. Pharmaceutics.* 2010; 7(1):60–74.
17. Cohen AL, Colman H. Glioma biology and molecular markers. *Cancer Treat Res.* 2015; 163:15–30. [PubMed: 25468223]
18. Faulkner C, Palmer A, Williams H, Wragg C, Haynes HR, White P, DeSouza RM, Williams M, Hopkins K, Kurian KM. EGFR and EGFRvIII analysis in glioblastoma as therapeutic biomarkers. *Br. J. Neurosurg.* 2014:1–7. [PubMed: 25141189]
19. Hatanpaa KJ, Burma S, Zhao D, Habib AA. Epidermal growth factor receptor in glioma: signal transduction, neuropathology, imaging, and radioresistance. *Neoplasia.* 2010; 12(9):675–684. [PubMed: 20824044]
20. Hegi ME, Rajakannu P, Weller M. Epidermal growth factor receptor: a re-emerging target in glioblastoma. *Curr. Opin. Neurol.* 2012; 25(6):774–779. [PubMed: 23007009]
21. Talasila KM, Soentgerath A, Euskirchen P, Rosland GV, Wang J, Huszthy PC, Prestegarden L, Skaftnesmo KO, Sakariassen PO, Eskilsson E, Stieber D, Keunen O, Brekka N, Moen I, Nigro JM, Vintermyr OK, Lund-Johansen M, Niclou S, Mork SJ, Enger PO, Bjerkvig R, Miletic H. EGFR wild-type amplification and activation promote invasion and development of glioblastoma independent of angiogenesis. *Acta Neuropathol.* 2013; 125(5):683–698. [PubMed: 23429996]
22. Chakravarti A, Chakladar A, Delaney MA, Latham DE, Loeffler JS. The epidermal growth factor receptor pathway mediates resistance to sequential administration of radiation and chemotherapy

- in primary human glioblastoma cells in a RAS-dependent manner. *Cancer Res.* 2002; 62(15): 4307–4315. [PubMed: 12154034]
23. Nakamura JL. The epidermal growth factor receptor in malignant gliomas: pathogenesis and therapeutic implications. *Expert Opin. Ther. Targets.* 2007; 11(4):463–472. [PubMed: 17373877]
  24. Wepler SA, Li Y, Dubois L, Lieuwes N, Jutten B, Lambin P, Wouters BG, Lammering G. Expression of EGFR variant vIII promotes both radiation resistance and hypoxia tolerance. *Radiother. Oncol.* 2007; 83(3):333–339. [PubMed: 17512071]
  25. Li Z, Zhao R, Wu X, Sun Y, Yao M, Li J, Xu Y, Gu J. Identification and characterization of a novel peptide ligand of epidermal growth factor receptor for targeted delivery of therapeutics. *FASEB. J.* 2005; 19(14):1978–1985. [PubMed: 16319141]
  26. Liu L, Mason RP. Imaging beta-galactosidase activity in human tumor xenografts and transgenic mice using a chemiluminescent substrate. *PLoS One.* 2010; 5(8):e12024. [PubMed: 20700459]
  27. Agnes RS, Broome AM, Wang J, Verma A, Lavik K, Basilion JP. An optical probe for noninvasive molecular imaging of orthotopic brain tumors overexpressing epidermal growth factor receptor. *Mol. Cancer Ther.* 2012; 11(10):2202–2211. [PubMed: 22807580]
  28. Urbanczyk-Pearson LM, Femia FJ, Smith J, Parigi G, Duimstra JA, Eckermann AL, Luchinat C, Meade TJ. Mechanistic investigation of  $\beta$ -galactosidase-activated MR contrast agents. *Inorg. Chem.* 2008; 47(1):56–68. [PubMed: 18072754]
  29. Bagshawe KD. Antibody directed enzymes revive anticancer prodrugs concept. *Br. J. Cancer.* 1987; 56(5):531–532. [PubMed: 3426915]
  30. Bagshawe KD. Antibody-directed enzyme prodrug therapy (ADEPT) for cancer. *Expert Rev. Anticancer Ther.* 2006; 6(10):1421–1431. [PubMed: 17069527]
  31. Senter PD, Springer CJ. Selective activation of anticancer prodrugs by monoclonal antibody-enzyme conjugates. *Adv. Drug Delivery Rev.* 2001; 53(3):247–264.
  32. Legigan T, Clarhaut J, Tranoy-Opalinski I, Monvoisin A, Renoux B, Thomas M, Le Pape A, Lerondel S, Papot S. The first generation of beta-galactosidase-responsive prodrugs designed for the selective treatment of solid tumors in prodrug monotherapy. *Angew. Chem. Int. Ed.* 2012; 51(46):11606–11610.
  33. Farquhar D, Pan BF, Sakurai M, Ghosh A, Mullen CA, Nelson JA. Suicide gene therapy using *E. coli* beta-galactosidase. *Cancer Chemother. Pharmacol.* 2002; 50(1):65–70. [PubMed: 12111114]
  34. Legigan T, Clarhaut J, Renoux B, Tranoy-Opalinski I, Monvoisin A, Berjeaud JM, Guillhot F, Papot S. Synthesis and antitumor efficacy of a  $\beta$ -glucuronidase-responsive albumin-binding prodrug of doxorubicin. *J. Med. Chem.* 2012; 55(9):4516–4520. [PubMed: 22515366]
  35. Tietze LF, Krewer B. Antibody-directed enzyme prodrug therapy: a promising approach for a selective treatment of cancer based on prodrugs and monoclonal antibodies. *Chem. Biol. Drug Des.* 2009; 74(3):205–211. [PubMed: 19660031]

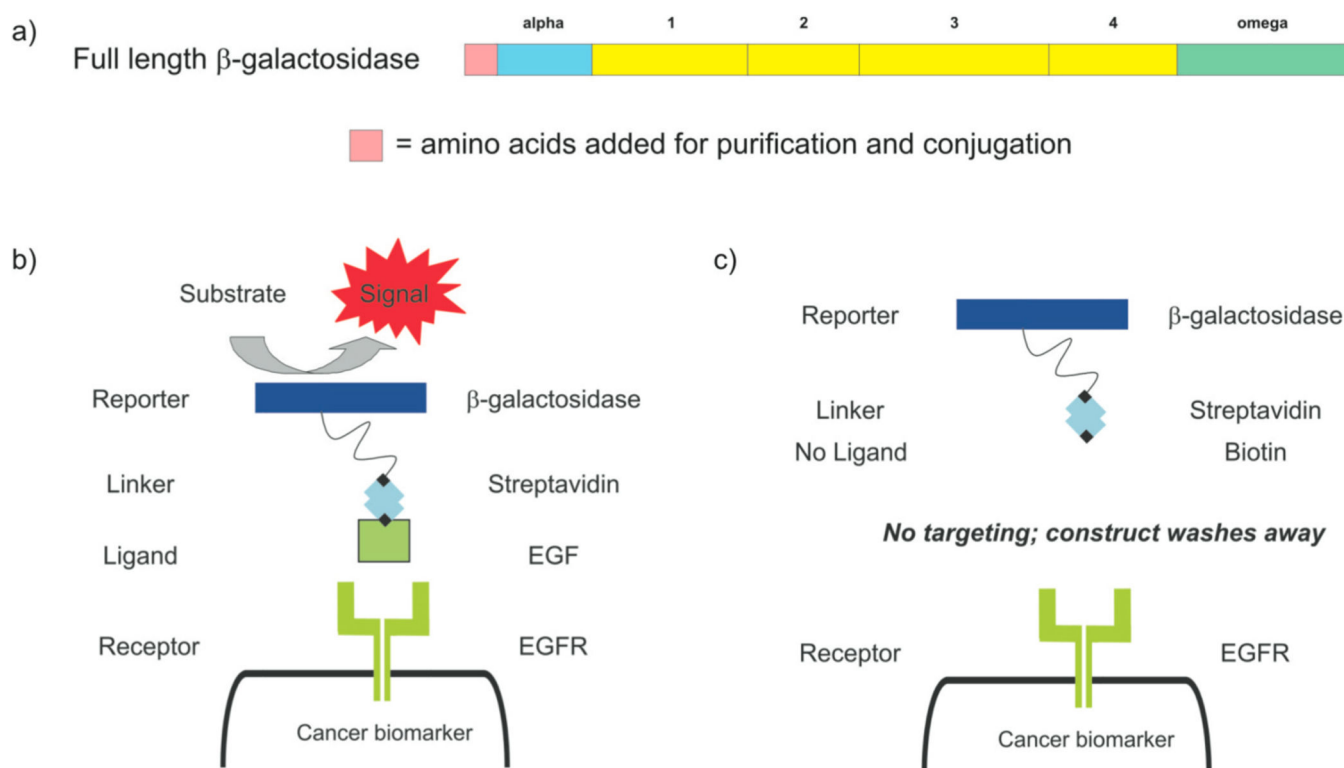


**Figure 1.** Engineering a reporter complex to identify cancer biomarkers exogenously. (a) Modified domains of full-length  $\beta$ -gal. (b) Targeted reporter activity. (c) Lack of reporter activity without targeting.

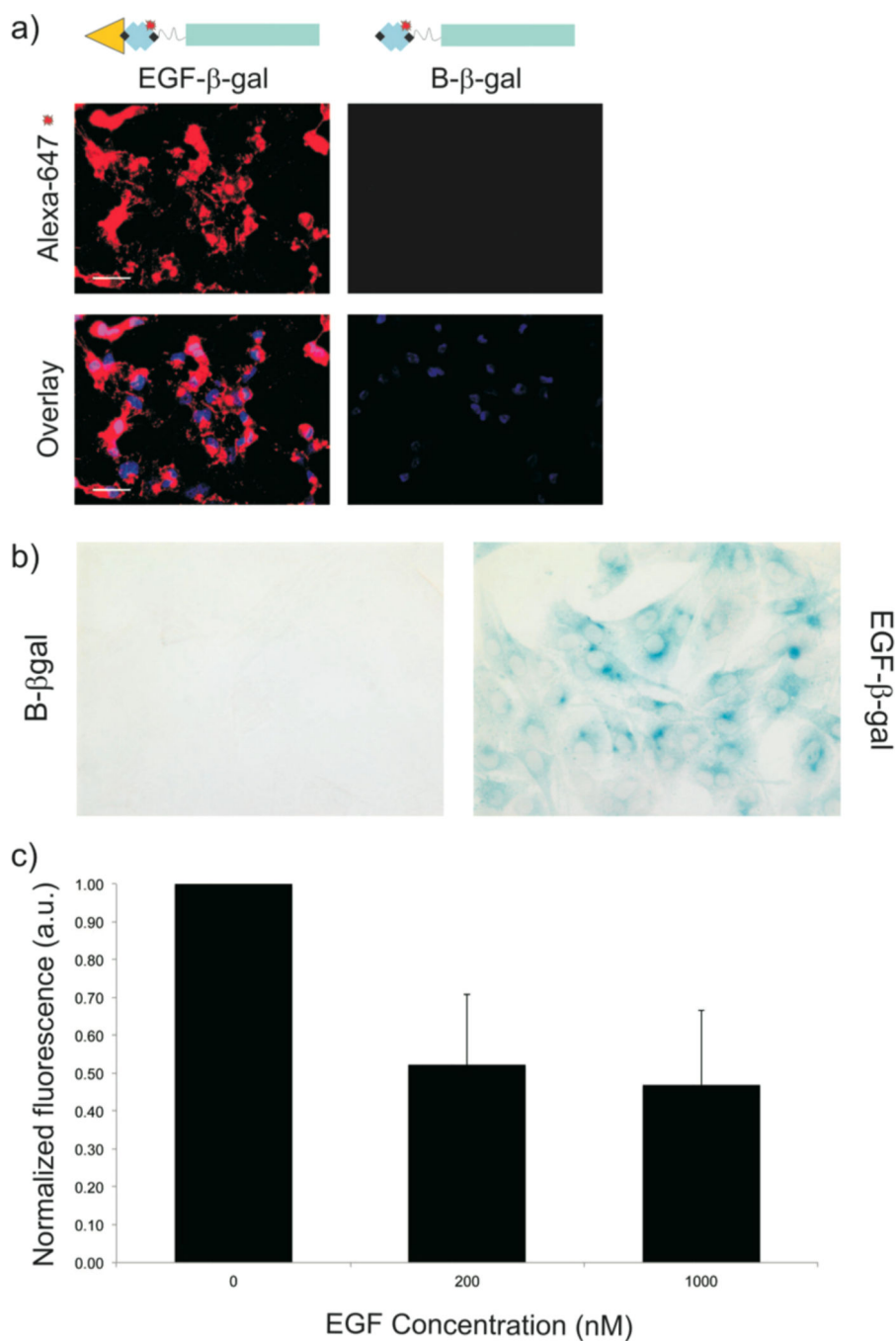


**Figure 2.**

In vitro activity of targeted- $\beta$ -galactosidase. (a) Gli36<sup>+</sup> cells incubated with either EGF- $\beta$ -gal or B- $\beta$ -gal were monitored by fluorescence microscopy using the fluorophore-labeled SA (647 nm) contained within the complex. (b) Internalized  $\beta$ -gal activity as shown by staining with the  $\beta$ -gal substrate, 5-bromo-4-chloro-3-indolyl- $\beta$ -D-galactopyranoside (X-gal). (c) Internalization of EGF- $\beta$ -gal was inhibited by full length EGF.

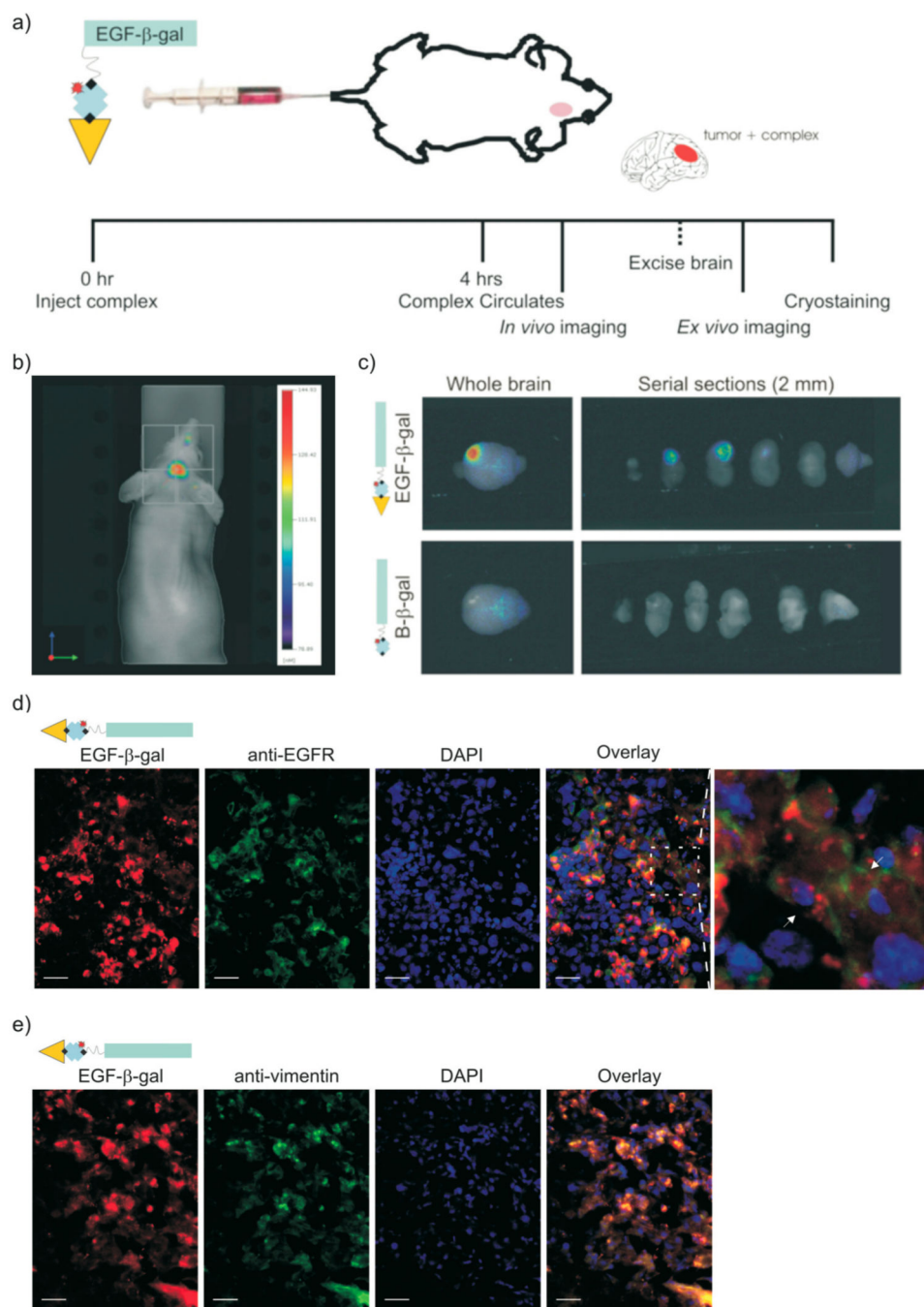


**Figure 3.** Fluorescence imaging of targeted-β-galactosidase complex in orthotopic brain tumors. (a) Flow chart of in vivo imaging for mice intravenously administered EGF-β-gal. FMT of a mouse with (b) orthotopic GBM administered EGF-β-gal ( $1 \text{ mg kg}^{-1}$  body weight) intravenously. The color bar represents the concentration (nM) of activated probe. (c) Mice containing implanted gliomas were administered EGF-β-gal or B-β-gal intravenously. The brains were then excised and imaged using in vivo multispectral fluorescence. (d,e) Excised

brains were cryosectioned and immunostained with anti-EGFR and anti-vimentin to demonstrate uptake localization of EGF- $\beta$ -gal.

Author Manuscript

Author Manuscript

Author Manuscript

Author Manuscript

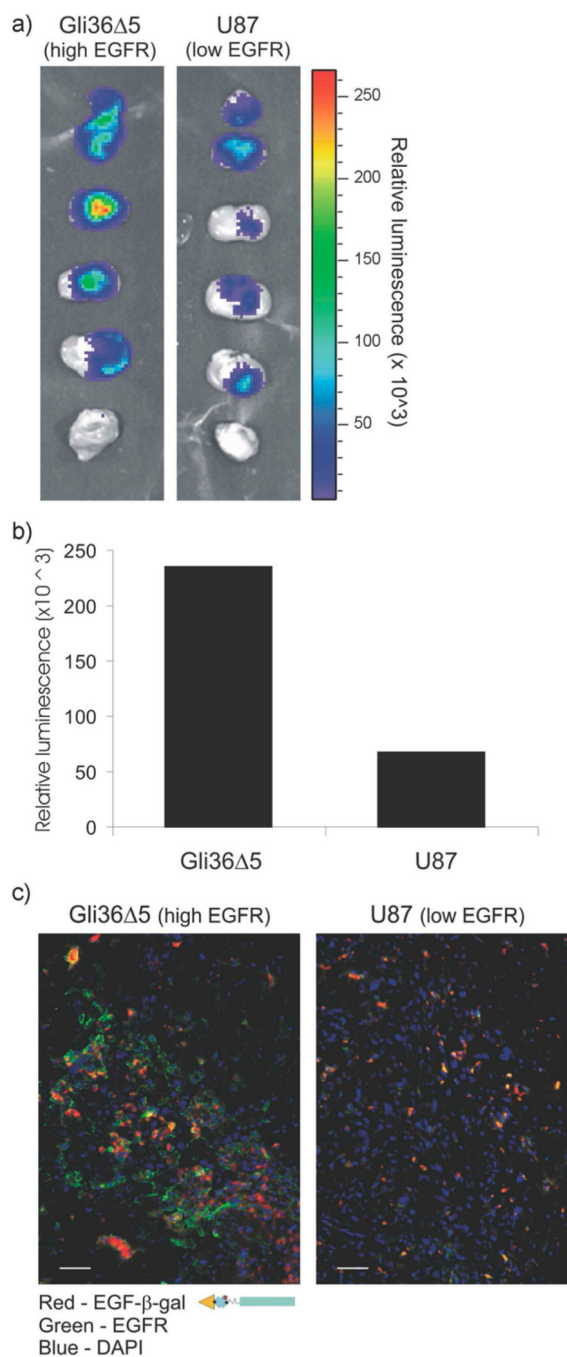


**Figure 4.**

Ex vivo bioluminescence imaging of targeted-β-galactosidase complex. (a) Mice containing implanted gliomas from Gli36 Δ5 or U87 cells were administered EGF-β-gal ( $1 \text{ mg kg}^{-1}$  body weight) intravenously. The brains were then removed and covered in Galacto-Light Plus, a bioluminescence substrate for β-gal. (b) Relative luminescence (photons per area per second) was calculated from each 2 mm brain slice and plotted. (c) Differential levels of EGFR expression were validated by immunostaining with anti-EGFR of cryosections from EGF-β-gal administered, tumor-containing brain.

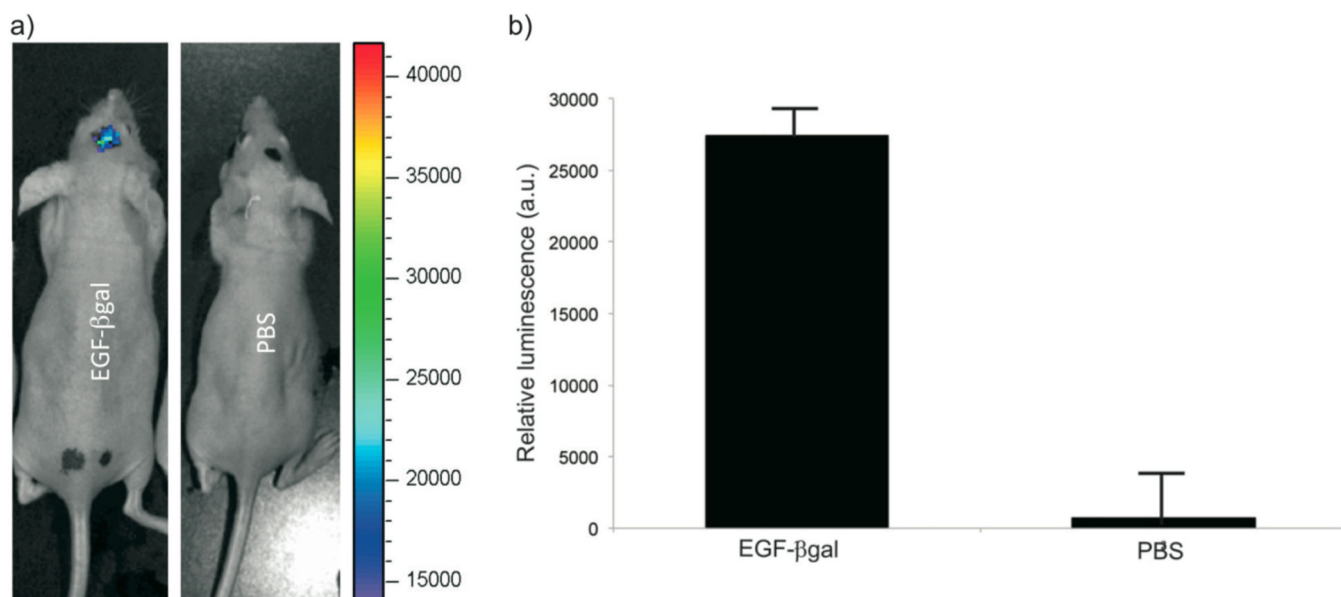


**Figure 5.** Bioluminescence imaging of targeted- $\beta$ -galactosidase complex in orthotopic brain tumors. Mice injected intravenously with either EGF- $\beta$ -gal ( $1 \text{ mg kg}^{-1}$  body weight) or sham saline were imaged after stereotactic administration of Galacto-Light Plus. Scale bar represents relative luminescence.